Accepted Manuscript

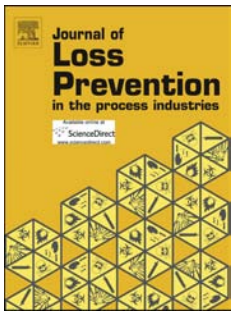

A new shock tube configuration for studying dust-lifting during the initiation of a coal dust explosion

David E. Gildfind, Richard G. Morgan

PII: S0950-4230(14)00034-5

DOI: 10.1016/j.jlp.2014.02.011

Reference: JLPP 2733

To appear in: *Journal of Loss Prevention in the Process Industries*

Received Date: 7 November 2013

Revised Date: 20 February 2014

Accepted Date: 23 February 2014

Please cite this article as: Gildfind, D.E., Morgan, R.G., A new shock tube configuration for studying dust-lifting during the initiation of a coal dust explosion, *Journal of Loss Prevention in the Process Industries* (2014), doi: 10.1016/j.jlp.2014.02.011.

- Experimental certification criteria for coal dust explosion suppression agents were identified.
- These test conditions were accurately reproduced in a shock tube.
- A new orifice plate concept was developed to maximum test time.
- The orifice plate permits practical location for test station.
- The orifice plate permits retrofit of larger outdoor facilities.

A new shock tube configuration for studying dust-lifting during the initiation of a coal dust explosion

David E. Gildfind[a], Richard G. Morgan[a]

[a] *Centre for Hypersonics, The University of Queensland, Room 50-C110 (Hawken Building), Cooper Rd, St Lucia, Queensland, 4072, Australia*

Abstract

The traditional defence against propagating coal dust explosions is the application of dry stone dust. This proven and effective safety measure is strictly regulated based on extensive international experience. While new products, such as foamed stone dust, offer significant practical benefits, no benchmark tests currently exist to certify their dust lifting performance in comparison to dry stone dust. This paper reviews the coal dust explosion mechanism, and argues that benchmark testing should focus on dust lifting during the initial development of the explosion, prior to arrival of the flame. In a practical context, this requires the generation of shock waves with Mach numbers ranging from 1.05 to 1.4, and test times of the order of 10's to 100's of milliseconds. These proposed test times are significantly longer than previous laboratory studies, however, for certification purposes, it is argued that the dust lifting behaviour should be examined over the full timescales of an actual explosion scenario. These conditions can be accurately targeted using a shock tube at length scales of approximately 50 m. It is further proposed that useful test time can be maximised if an appropriately sized orifice plate is fitted to the tube exit, an arrangement which also offers practical advantages for testing. The paper demonstrates this operating capability with proof-of-concept experiments using The University of Queensland's X3 impulse facility.

Keywords: coal dust explosion, stone dusting, low Mach number blast wave, shock tube, orifice plate

[1]Corresponding author: David E. Gildfind
[2]Email: d.gildfind@uq.edu.au
[3]Telephone: +61 (0)7 3365 1065

1. Introduction

Underground coal mines are immersed in coal dust, which is produced during the cutting, moving, and processing of coal in the mine (Harris et al., 2010). This dust, which can float through the mine many metres away from its source, settles onto horizontal surfaces such as walkways, work surfaces, shelving, overhead surfaces, and so forth. In the confined spaces of a coal mine, a coal dust explosion may occur when these fine particles of coal are raised into the air and in some way are ignited (Humphreys & OBeirne, 2000). The source of this ignition is termed the initiator.

The normal initiator for a coal dust explosion is the accidental ignition of methane, a gas which is produced during the mining of the coal, and like the coal dust itself, is ever-present in coal mines (Cybulski, 1975). A methane explosion can be responsible for both raising a dangerous cloud of coal dust, and at the same time, providing the heat required to ignite the dust cloud (Cybulski, 1975). Other potential initiators include shot firing, friction sparks, electrical arcing, and naked flame, although these must be coupled with a ventilation/wind source to initially raise the coal dust into the air (Cain, 2003). When a volume of methane ignites within the confined space of the mine, a shock wave is propagated ahead of the flame front. Air between the shock and the flame front has induced velocity which causes it to raise the coal dust, and mix it with air into explosive conditions. A propagating explosion begins when the trailing flame ignites the lifted coal dust. As Humphries and O'Beirne (Humphreys & OBeirne, 2000, pg. 1) note:

> *"Until there is a break in this cycle of raising then igniting coal dust, the explosion continues to propagate, generating destructive pressures and large quantities of irrespirable and toxic gases. Ultimately, a coal dust explosion could pass through the entire coal mine until it reached the surface."*

Coal dust explosions fall under the more general category of dust explosions; Figure 1 from Sichel et al. (Sichel et al., 1995) details the stages involved in a dust explosion. It can be seen that in the most powerful dust explosions the pressure and temperature rise from the shock itself are sufficient to combust the coal dust/air mixture (Sichel et al., 1995), resulting in a detonating explosion, however it is thought that this mode has not occurred in any real-life coal mine explosions (Cybulski, 1975; Oberholzer, 1997). Even if

the initial explosion of methane is a relatively minor event by itself, the propagating coal dust explosion which ensues may be a truly devastating event. *"Miners frequently survive gas explosions; they rarely survive explosions in which coal dust has a major involvement"* (NSW DPI, 2001, pg. 4).

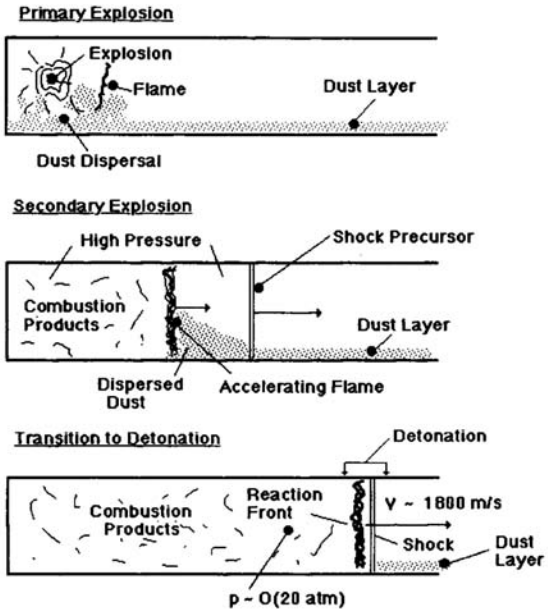

Figure 1: Elements of a layered dust explosion (reproduced with permission from Sichel et al. (1995, Figure 1)).

2. Stone dusting

The primary defence against propagating coal dust explosions is stone (or rock) dusting. First employed in the early 20th century, this involves distributing a layer of stone dust, typically limestone, over working surfaces exposed to coal dust (Cain, 2003). During an explosion, the stone dust disperses into the air, mixes with coal dust, and prevents propagation of the explosion flame through the coal dust (Man & Teacoach, 2009).

Stone dust acts as a thermal inhibitor/heat sink (Man & Teacoach, 2009), absorbing energy from the system, blocking coal particles from radiation arising at the flame front and therefore reduces preheating of the coal, and can reduce flame temperature such that devolatilisation no longer occurs in the

coal particles (Cashdollar et al., 2010; Cybulski, 1975; Dastidar et al., 1997; Harris et al., 2010; Man & Teacoach, 2009). In sufficient quantities stone dusting will completely prevent explosion propagation (Cashdollar et al., 2010).

The amount of stone dust which is required to suppress the explosion of a cloud of coal dust can be defined in terms of the Total Incombustible Content (TIC) of the coal dust/stone dust mixture. The higher the TIC, the greater the stone dust content in the mixture. The minimum TIC to suppress an explosion depends on the explosibility of the coal dust, which varies with the type of coal (which itself is unique to each geographical mine site), and the condition of the coal dust (for example, the particle size, the internal surface area, moisture content, and so forth (Cain, 2003; Woskoboenko, 1988)). The explosibility of a given coal dust, and the minimum TIC to suppress its explosion, can both be established in the laboratory setting (Woskoboenko, 1988).

However, within a practical mine setting, sufficient stone dust must be applied so that the *raised dust cloud* has the required minimum TIC, not simply the aggregate surface dust, and that it is adequately mixed. Figure 2 shows an example of fine float coal dust resting on top of a thick layer of stone dust. Float coal dust refers to coal particles capable of floating through the mine workings, and are generally considered to consist of particles of coal smaller than 75 microns (NIOSH, 2006).

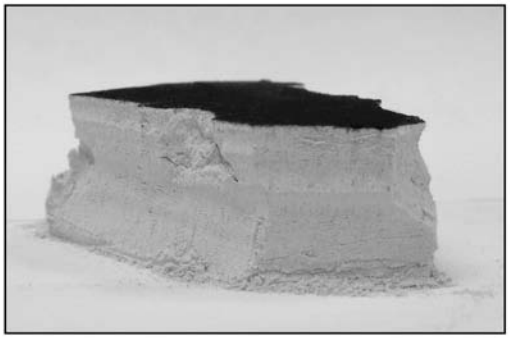

Figure 2: 0.025 mm of float coal dust deposited on top of 20 mm of stone dust (reproduced with permission from NIOSH (2006)).

The Office of Mine Safety and Health Research (OMSHR) notes that *"layering of coal dust on top of rock dust can defeat all rock dusting efforts"*

(OMSHR, 2014); even a thin layer of float coal dust, which can be raised by a relatively weak initiating explosion, can support a propagating coal dust explosion. For typical mine dust, in a typical mine setting, the minimum thickness of coal dust on the floor required to support an explosion may be as little as 0.05 mm (Cain, 2003; NSW DPI, 2001). However, considering a typical mine, foot prints in the coal dust would normally be unobservable until the dust was significantly thicker than 0.1 mm; visible foot prints indicate sufficient coal dust to propagate an explosion (Stephan, 1998).

A weak initiator, while capable of raising float coal dust, may only be powerful enough to scour just the upper surface of any underlying stone dust. Weak explosions associated with float coal dust are normally assumed to strip only a thin layer of floor dust away, typically 2–4 mm (Cain, 2003; Harris et al., 2010; Humphreys & OBeirne, 2000; NIOSH, 2006). To ensure sufficient inert content within the *raised dust cloud*, it is therefore necessary to repeatedly apply stone dust so that the top few millimetres of surface dust thickness (i.e. the thickness of dust that will actually be scoured by the explosion front) meets minimum TIC requirements. Referring to Figure 2, most of the observed through-thickness stone dust is therefore unlikely to contribute to the suppression of a weak explosion.

The problem of float coal dust drives the stone dusting process within mines, and has significant practical implications on mining operations. The conventional method of distributing stone dust is to spray dry stone dust onto surfaces exposed to coal dust. To prevent exposure to airborne dust, personnel must be extracted while the dust remains airborne. As a result there can be large delays to production before the air clears (Mining Mirror, 2013).

Slurry (or wet) stone dusting involves mixing water with the stone dust before spraying it (OMSHR, 2014), and can avoid the production delays associated with dry stone dusting. Oberholzer et al. (2005) conducted a detailed review of slurry dusting and arrived at a number of conclusions, including the following:

- The slurry dust was effective at gathering and capturing existing coal dust. It was also much more effective than dry stone dust at adhering to inclined surfaces such as the walls and ceiling of the mine.

- The slurry dust dried after about four days, at which time it had a similar moisture content to stone dust which had been applied dry.

However, despite having the same moisture content, the slurry dust was observed to 'cake', whereas the other dust remained loose and much more easily dispersed.

- Significant force was required to break up and raise the caked slurry dust. In the event that the caked slurry dust would fragment, the particle size was much larger, and would therefore be less effective at explosion suppression.

Oberholzer et al. (2005) recommended against using slurry dust in locations where there was a high rate of coal dust deposition, since the underlying caked stone dust could not be relied upon to inert the continuously accumulating upper layer of coal dust. NSW DPI (2001) only approves of slurry dusting at the beginning of a dusting campaign, and states that it must be followed by ongoing treatments with dry stone dust. The OMSHR (2014) similarly regards wet stone dusting as ineffective at explosion suppression.

In their review of slurry dusting, Oberholzer et al. (2005) examined what testing would be required to assess the suitability of slurry dust as a replacement for dry stone dust. They argued that the goal of any testing should be to expose a sample of slurry dust to an air blast representative of an actual explosion, and then to determine the properties of the raised stone dust cloud, in terms of amount and composition of the raised stone dust particles. They also argued that enough was already known about the explosibility of coal and stone dust mixtures that further explosibility testing with slurry dust was not necessary.

New products are emerging which can be used to transform a water and stone dust slurry into a foam (Mining Mirror, 2013). Additives are first mixed into the slurry, then it is injected with compressed air. The foaming stone dust has similar operational characteristics to traditional slurry dusting, except that the foam does not cake when it dries (Mining Mirror, 2013). In theory such products can be scoured during an explosion (OMSHR, 2014), and therefore could potentially replace dry stone dust as a defence against float coal dust.

While products such as foaming coal dust potentially offer a significantly improved alternative to dry stone dusting, there are currently no clear guidelines for certifying the efficacy of such products in place of traditional dry stone dust, which is already known to work. The OMSHR notes that *"no required testing of these additives currently exists to determine if they function*

properly and if they are equivalent in behaviour to a dry rock dust application" (OMSHR, 2014).

3. Aims of this Study

The present study had two aims. The first aim was to establish suitable benchmark tests to address the issues regarding the certification of new methods of stone dust deposition, as identified above by the OMSHR (OMSHR, 2014). After establishing a rational set of requirements for such testing, and identifying the critical test cases, the second aim was to optimise the configuration of a shock tube for the accurate reproduction of these benchmark test flows, in terms of velocity, pressure, flow quality, duration, and test section location.

In addressing the second aim of this study, it was shown that large scale shock tubes can produce blast waves which are representative of actual mine explosion scenarios, even though no coal dust or combustion processes are present. Additionally, a new orifice plate concept is proposed which can significantly increase the blast wave duration, permits the test flow to be exhausted into atmospheric pressure, and provides practical benefits such as convenient test station positioning (i.e. where the dust sample would initially be located) and convenient management/collection of experiment waste products (where the scoured dust will be exhausted).

In this paper, the arguments of Oberholzer et al. (2005) have been extended to stone dust products generally, such as slurries or foams. Stone dust 'products' shall refer to different techniques of applying stone dust. If the constituent stone dust of a given product is already approved for use, then it will be assumed that benchmark tests do not need to re-establish the explosibility properties. It should then be possible to demonstrate the efficacy of a new stone dust product by comparing it to dry application of the same stone dust, in terms of:

- The amount of stone dust which is raised.
- The composition of the raised stone dust.
- The mixing of the stone dust.

These properties should be measured for the new stone dust product after it has been exposed to a blast wave which is representative of an actual coal

dust explosion. The key to this approach is to identify the critical explosion case, or cases. The benchmark test flow should reproduce the flow properties of the air blast *preceding* the flame during an actual explosion; this is the time when dust lifting and mixing must take place effectively for the ensuing flame to be extinguished. The duration of this blast of gas should be equivalent to the actual explosion, in order to provide a realistic time frame for dust lifting and mixing to occur.

It will be argued in this paper that testing should consider the *weakest* explosions that will likely occur, since this presents the most challenging scenario for dust lifting and mixing. In stronger explosion scenarios the dust lifting performance will be at least that of the weak explosion case.

If equivalent dust lifting and mixing performance can be be established for a new stone dust product, then its functional behaviour and equivalence to the corresponding dry stone dust should have been achieved, thus addressing certification issues as identified by the OMSHR (OMSHR, 2014).

4. Existing Test Facilities

Stone dusting is a heavily regulated process, with prescriptive requirements that have evolved over the last century. Regulations are conservative, and based on significant accumulated international experience. As noted previously, laboratory experiments are used to establish the explosibility of specific coal dusts with different levels of TIC. However, to simulate the more complex coal dust propagating explosion process, detonation tubes are used. Examples include the Kloppersbos facility in South Africa (Humphreys et al., 2010), or the SIMTARS facility in Australia (Wu et al., 2009). Experimental mines have also been developed to study propagating coal dust explosions within a realistic mine layout; for example the Lake Lynn Experimental Mine (LLEM) in Pennsylvania is a former limestone mine which has multiple drifts and cross-cuts, and can perform full-scale explosion testing (Sapko et al., 2000) .

Considering detonation tubes, a schematic of the 200 m long, 2 m diameter Kloppersbos detonation tube is shown in Figure 3. An atmosphere of methane gas is initially contained between a thin film diaphragm, and the closed end of the tube (the left side of Figure 3). Two 30 m long zones of coal dust are established down the length of the tube. When the methane is ignited, a propagating explosion is produced in the first coal dust zone. Stone dust may or may not be added to the second zone of coal dust. The

facility can be used to demonstrate a propagating explosion, or to determine the amount of stone dust which must be added to the second zone of coal dust in order to extinguish the propagating explosion. Experimental mines are functionally similar to detonation tubes, but provide even more realistic explosion simulation, and facilitate testing of other mining hardware, such as explosion barriers and seals.

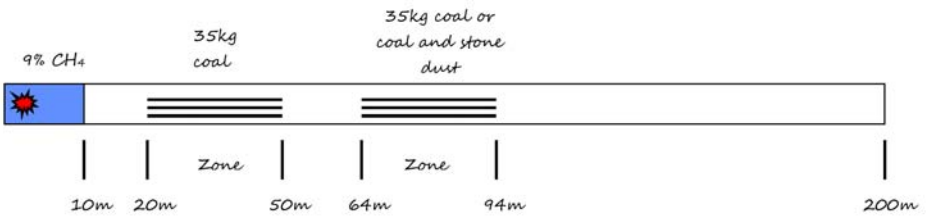

Figure 3: Schematic of the Kloppersbos detonation tube, Pretoria, South Africa (reproduced with permission from Humphreys et al. (2010)).

Detonation tubes and experimental mines provide a practical basis for establishing stone dusting guidelines with respect to different mining scenarios, and also offer a powerful training tool to demonstrate the devastating effect of an actual coal dust explosion (refer Figure 4). However, these large and explosive facilities do not presently offer the opportunity for detailed studies of the dust lifting process. Referring to Figure 1, critical stone dust lifting processes take place during the period of steady flow which occurs between the passing of the shock wave, and the arrival of the flame.

Both of these types of facility use methane to initiate a propagating coal dust explosion, have complex flow and combustion processes, and are not readily configured to precisely reproduce the flow conditions prior to flame arrival. Furthermore, these structures are designed for high loads and a harsh internal environment, and are poorly suited for instrumentation required to conduct a detailed examination of the dust lifting process. These facilities are large and expensive to operate, and introduce additional safety issues which must be managed.

Considering the certification of new stone dust products, detonation tubes and experimental mines can provide a final independent validation of the product. These tests can establish whether or not a new product can suppress one of the standard propagating coal dust explosions which these facilities generate. However, such tests do not readily demonstrate, in detail,

Figure 4: Demonstration of a propagating coal dust explosion at the Kloppersbos facility (reproduced with permission from Humphreys et al. (2010)).

the relative performance of different products, and therefore cannot establish equivalence between new and existing stone dust application techniques. These tests only address a limited range of explosion scenarios, and do not establish the performance of stone dust products for the *weakest* explosion scenarios. Finally, they also generate complex wave processes (for example, rarefractions and organ pipe oscillations (Singer et al., 1976)) which complicate the interpretation of results. As such, they form an insufficient basis for certification by themselves.

Several studies have examined dust lifting behind a shock wave using a shock tube. This is a tube which initially has a high pressure driver gas separated from a lower-pressure test gas by a diaphragm. When the diaphragm is ruptured, a shock wave propagates into the test gas, and an expansion wave propagates into the driver gas. Shock-processing compresses and heats the test gas, and induces a mass motion of the test gas towards the direction of the shock (Anderson Jr., 1990). These are the same conditions which precede the flame front during a propagating coal dust explosion.

Before secondary wave processes arrive, the shock speed, and the flow conditions behind the shock, are initially steady and can be accurately adjusted based on shock theory, especially at low Mach numbers. The size of a shock tube is a critical factor affecting its performance; the longer the tube, the longer the test gas slug, and therefore the longer the duration of useful test time; the wider the tube, the larger the test sample which can be tested.

Previous shock tube studies have focussed on improving understanding of the mechanism of dust lifting and to improve physical modelling of these processes. Example studies include Gerard (1963); Klemens et al. (2006); Marks et al. (2013); Suzuki et al. (2005). These experiments have examined

the response of dust immediately after the passing of the shock wave, and have used shock tubes up to 6 metres total length (including driver tube, driven tube, and test section). These length scales can provide steady test flows of up to a few milliseconds. None of these experiments were intended to provide certification data to distinguish different stone dust products for direct application in mining operations, and the short test times are considered insufficient for the testing proposed in this paper. However the instrumentation and visualisation techniques used in these studies would have direct application to the larger scale shock tube experiments proposed in this paper.

In their review of slurry dusting, Oberholzer et al. (2005) blasted a jet of compressed air over dry stone dust and slurry dust samples. The rationale was to scour a dust sample that would be representative of that scoured by an actual explosion. The jet velocity was adjusted to match dynamic pressures of between 0.1 and 2.5 kPa. This dynamic pressure range was calculated to correspond to air velocities of between 10 and 64 m/s respectively, which were considered to model weak explosion scenarios. The duration of the jet blast was not stated, however it is assumed that the jet was operated for a number of seconds, and not operated impulsively.

It is argued in this paper that the approach of Oberholzer et al. (2005) has merit because it targets weak explosions, and it attempts to assess the stone dust product by measuring its response to the blast of shock-processed air preceding the arrival of the flame, which is when effective dust mixing must occur. However, it is believed that a shock tube can simulate these conditions more effectively, for three reasons: firstly, the shock tube reproduces shock wave interaction with the dust sample; secondly, the shock tube can accurately reproduce the static pressure rise and other flow properties behind the shock; and thirdly, a sufficiently long shock tube can achieve representative timescales.

5. Required Test Conditions

Given that a shock tube would be optimised for this study, it was first necessary to precisely define the required test conditions. The aim of the present study was to realistically reproduce the flow conditions which occur between the shock and the flame, with a focus on using these conditions to study the processes associated with explosion *suppression*. The actual conditions this entails clearly depend on the characteristics of the explosion, which can vary in terms of Mach number, velocity, duration, and so forth. However,

since the stated emphasis here is explosion suppression, then the most important conditions to reproduce in the laboratory are those associated with *weak* explosions.

The justification for this assertion is that even strong propagating explosions are likely to *begin* as weak explosions, which then progress to strong explosions. Oberholzer et al. (2005) note that the large efforts made to eliminate explosion hazards in modern mines are such that if a methane explosion is actually to occur, it is most likely to be weak in nature. Furthermore, effective dust lifting is most challenging at the lower velocities and static pressures associated with weaker explosions. Finally, the most logical and effective time to suppress an explosion is as soon as possible after its formation, if the initial explosion formation cannot itself be avoided.

Cybulski (1975) characterises weak propagating coal dust explosions as having shock wave velocities ranging between 360 and 460 m/s, and an associated static pressure rise of between 10 and 40 kPa. This corresponds to an approximate shock Mach number of between 1.05 and 1.3, behind which the induced velocity of the air ranges between 28 and 169 m/s. This is generally consistent with NSW DPI (2001) and Liebman et al. (1979), although Stephan (1998) states that in most realistic explosion scenarios the wind speed behind the shock actually exceeds 90 m/s. Cybulski (1975) notes that these weak explosions tend to either fade away or increase in strength. However, since the primary cause of propagating explosions is a (relatively) weak methane initiator explosion (unless a large volume of methane ignites (Cybulski, 1975)), most real explosions begin as weak explosions.

A weak initiator by itself will not necessarily cause a propagating explosion through sodden wet coal dust (Cybulski, 1975), or coal dust comprised of larger particles, or coal dust with low volatile content (NSW DPI, 2001). However, a *weak* propagating coal dust explosion is much more powerful than the methane explosion which triggered it; as such, the resulting coal dust explosion may now be considered a *strong initiator*. This initial coal dust explosion may now be able to propagate through a region of coal dust which would not explode with just the weaker initiator by itself (NSW DPI, 2001). Furthermore, 'pressure piling' can also occur since the coal dust suspension ahead of the flame can undergo significant compression prior to ignition (Abbasi & Abbasi, 2007; Sapko et al., 2000). These factors all result in a tendency for explosions to become stronger as they progress, unless suitable retardant techniques are applied.

Since the present study has focussed on recreating the post-shock flow

conditions associated with weak explosions, it has targeted shock waves with Mach numbers between 1.05 and 1.4. While defining the required shock Mach number also defines the required flow conditions behind the shock, it does not establish the required test time. In order to assess the effectiveness of different stone dust products within an actual mine explosion scenario, it is important to establish how much time is available, in an actual mine explosion scenario, for the dust to lift and mix prior to the arrival of the flame. After this point in time, the flame will have arrived, and if insufficient stone dust has lifted, and if mixing with coal particles is inadequate, the stone dust will not prevent entrained coal dust particles from igniting.

Dust lifting is not instantaneous; studies such as Gerard (1963) and Klemens et al. (2006) have shown that after the shock wave passes over a dust layer, there is a delay prior to the dust beginning to lift, and there is then a timescale associated with the dust mixing and reaching its maximum height. These processes were shown to occur over longer timescales at slower shock speeds (Klemens et al., 2006). Experimental testing aimed at certification of new stone dust products should provide sufficient time for dust to lift and mix. This 'test time' should be based on the timescales of realistic explosion scenarios; if the test time is too short, the full extent of dust lifting and mixing may be underestimated; if the test time is too long, the performance of the product may correspondingly be over-estimated. Whether or not this 'test time' is critical could, however, be established through experimentation.

The required test time cannot be strictly defined, but representative values can be derived by an examination of realistic mine explosion scenarios. Considering the secondary explosion in Figure 1, the time duration between the passing of the shock and the arrival of the flame depends on the shock and flame speeds (which are a function of shock Mach number), and the distance the shock has travelled since its formation (which depends on the distance away from the explosion source). Therefore, the wind behind the shock, which lifts the coal and stone dust into suspension, will have increasing duration with increasing distance away from the initial explosion source.

Stone dusting is typically not required right up to the cutting face. In the US rock dust must be applied within 40 ft (12 m) of the cutting face (Cashdollar et al., 2010); inside this 40 ft zone coal dust must be removed before it accumulates, and water (or a similarly effective agent) must be used to settle airborne dust (Cashdollar et al., 2010). Similarly, several other countries require application of stone dust stone dust no further than 10 m away from the active coal face (Cain, 2003; Cybulski, 1975). Considering the

shorter 10 m length, this requirement can be used to establish a representative timescale for testing of stone dusting products.

If it is then assumed that an initiator explosion occurs at the coal face itself, the time separation between the arrival of the shock front and the expanding combustion gases can be calculated from simple shock wave theory across this 10 m length. This time duration, which is a function of the driven shock Mach number, is the time available for the stone dust to adequately mix with the core flow before the flame arrives. If the stone dust does not satisfactorily mix within this time it will not work, and a propagating coal dust explosion may be initiated. Figure 5 summarises the required test conditions based on a shock Mach number of 1.05–1.4, and an ideal gas analysis. Test time is calculated for a position 10 m away from shock formation.

6. Experimental Setup

The non-reflected shock tube is an appropriate tool for creating the flow conditions detailed in Figure 5. The driver requirements are not extreme, and can easily be met using room temperature compressed air. The available test time will depend on the length and diameter of the facility, and tuning the wave processes to locate the test section at the optimum point. The X3 superorbital expansion tube at The University of Queensland is 62 m long, has a driven tube diameter of 182.6 mm, and is a suitable platform for such experiments (although it was not specifically designed for such conditions). For this study, the last 29 m were used, with the driver section being 12.5 m long, and the shock tube 16.5 m, as shown in Figure 6.

For the termination of the shock tube, there are two conventional configurations. The shock tube may open out into a large dump tank to receive the shock processed gas, or a fixed end boundary condition may be imposed, creating a 'reflected' shock tube. Due to the low shock Mach numbers relevant to this study, the post-shock flow is subsonic. Therefore the downstream boundary condition is important, and may send perturbations back upstream which reduce the test time at the observation station. Since the reflected shock travels back up the tube faster than the unsteady expansion fan created with the open end condition, it will terminate the flow earlier. So the open ended, non-reflected, configuration was chosen for these tests. The resulting x-t diagram is shown in Figure 6a.

In Figure 6a the point of maximum test time is where the unsteady $u - a$ wave intersects the interface (between driver gas and test gas), and is marked

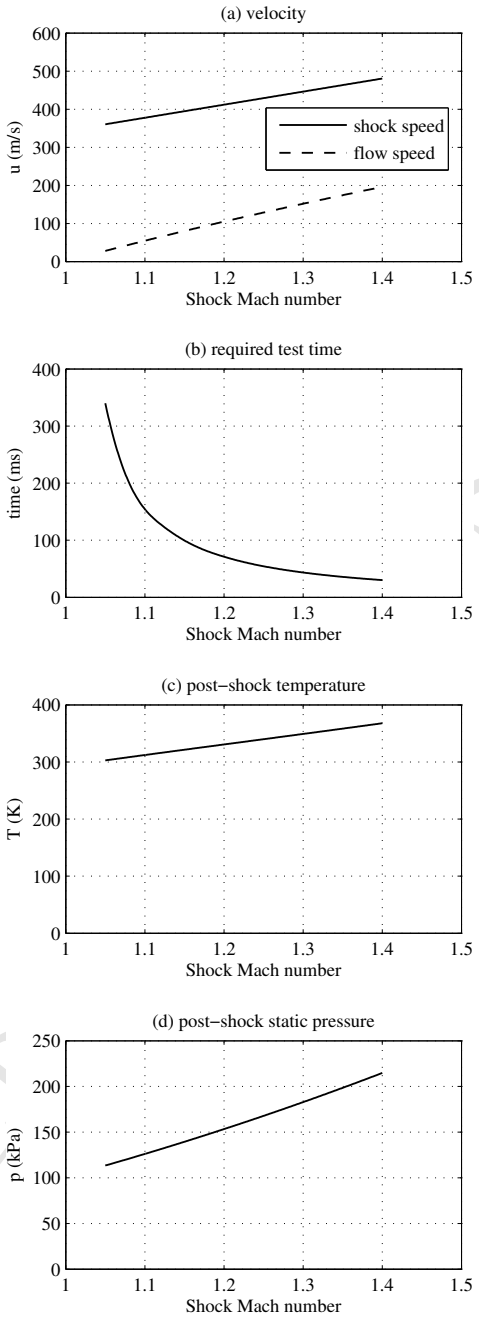

Figure 5: Summary of required test flow properties to assess stone dust lifting by weak explosions. Required test time is calculated based on a 10 m distance from the explosion source.

by the symbol Δt_{max} on the figure. u and a are the local flow velocity and local sound speed respectively, and a $u - a$ wave is a wave travelling *against* the direction of the flow. The location of maximum test time is dependent on the shock speed, and corresponds approximately to the location of the pressure transducer $at3$. For the downstream boundary condition, Δt_{max} is the station where it would be most appropriate to locate the test section. A test section would likely consist of a set of windows for high speed flow visualisation, an interior platform to locate dust samples, and instrumentation as required by the specific testing. Note, the tests detailed in this paper were conducted to establish optimum configuration of the shock tube facility to conduct dust lifting experiments with the new benchmark test flows; actual testing of dust samples will require modifications to the facility in accordance with the findings and recommendations of this study.

Referring to Figure 6a, it is clear that the last 6 m of the tube do not directly add to the available test time, but are instead required to delay the arrival of the upstream propagating $(u - a)$ waves until the useful test gas runs out. In order to cancel the effects of the $u - a$ wave, and to use the full length of the tube to create useful test flow, an 'orifice plate' has been designed to fit across the downstream end of the shock tube; refer Figure 6b. If the area of the orifice is correctly chosen, the reduced mass flow rate through the sonic throat will exactly match the mass flow behind the shock, and no waves will reflect back upstream to corrupt the flow at the test station. Also, because the sonic throat in the orifice precludes propagation of information back upstream into the shock tube, the downstream conditions in the dump tank become decoupled from the shock tube, and there will be no upstream influences until after the test flow has ended. There is a starting process associated with establishing the flow through the orifice, and minor disturbances from this will propagate back upstream and be seen as noise at the test station. Whether or not this is important will depend on the nature of the tests being conducted.

For the fixed end boundary condition, a strong reflected shock propagates back upstream. For the open ended condition, a strong expansion wave propagates back upstream. The orifice plate can be considered to create a balanced condition, where the two effects cancel out. Figure 7 shows the required orifice area ratio, A/A^* as a function of *shock* Mach number, and is calculated by substituting the *post-shock* flow properties (region 2 in Figure 6b) into the ideal gas area-Mach relation (refer Anderson Jr. (1990), Eq. 5.20) as follows:

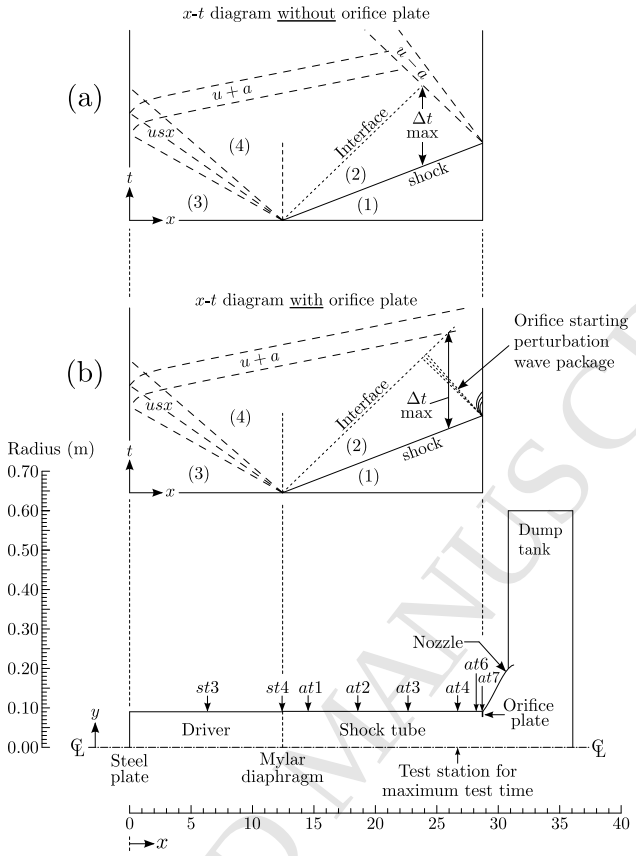

Description	x (m)	y (m)
LH wall	0.0	-
Transducer $st3$	6.351	0.090
Transducer $st4$	12.435	0.090
Mylar diaphragm	12.465	-
Transducer $at1$	14.535	0.0913
Transducer $at2$	18.593	0.0913
Transducer $at3$	22.658	0.0913
Transducer $at4$	26.722	0.0913
Transducer $at6$	28.323	0.0913
Transducer $at7$	28.752	0.0913
Orifice plate tip	28.777	0.077
Nozzle inlet plane	28.827	-
Nozzle exit plane	31.417	-

Figure 6: Layout of shock tube with orifice plate installed, test station located at $at4$. Horizontal scale has been compressed for clarity. In the figure, *usx* is an abbreviation for *unsteady expansion*; $u + a$ indicates a wave travelling at a speed equal to the local flow velocity, u, *plus* the local sound speed, a (i.e. a wave travelling in the direction of the flow); $u - a$ indicates a wave travelling at the local flow velocity, u, *minus* the local sound speed, a (i.e. a wave travelling against the flow).

$$\left(\frac{A}{A^*}\right)^2 = \frac{1}{M_2^2}\left[\frac{2}{\gamma+1}\left(1+\frac{\gamma-1}{2}M_2^2\right)\right]^{(\gamma+1)/(\gamma-1)} \quad (1)$$

where γ is the ratio of specific heats for air, and M_2 is the Mach number of the flow behind the shock.

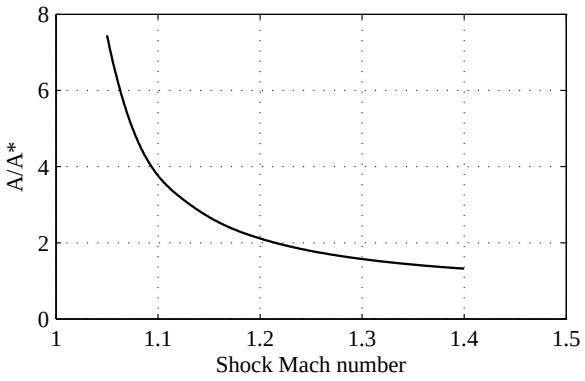

Figure 7: Required area ratio to achieve sonic flow through orifice plate, in terms of *shock* Mach number. A/A^* is the ratio between the driven tube area and orifice area.

7. The Experiments

Proof of concept tests were run at a range of conditions with the shock tube venting directly into the dump tank, then an orifice plate was designed to match a representative condition, and its satisfactory operation was demonstrated by two more shots using the orifice. The shots performed, and the resulting shock speeds and test times are given in Table 1. It is noted that these experiments relied on spontaneous rupture of the Mylar diaphragm under driver pressure loading. The pressure at which the diaphragm ruptured had to be established experimentally and had some variability, so achieving the required driver pressure was an iterative process. Therefore, while Shots #6 and #7 in Table 1 each used the same orifice area ratio, the orifice was only effectively 'tailored' for Shot #7. However, a future test campaign would use a rupturing device to initiate diaphragm rupture at a precisely defined driver pressure.

Table 1: Shot summary. Test time begins upon shock arrival and terminates when either the [1]driver gas interface arrives (calculated using L1d), or [2]the test flow pressure drops significantly.

	Fill pressure						
Shot ID	Driver tube (kPa)	Shock tubes (kPa)	Avg. shock speed (m/s)	Avg. shock Mach	Post shock speed (m/s)	Test time (ms)	Orifice plate?
1	485	75	490	1.42	204	25[1] ($at3$)	No
2	355	90	450	1.30	153	41[2] ($at3$)	No
3	160	91	389	1.12	67	36[2] ($at3$)	No
4	205	81	416	1.20	106	38[2] ($at3$)	No
5	285	81	443	1.28	143	40[2] ($at3$)	No
6	265	80	439	1.27	138	62[1] ($at4$)	Yes
7	260	58	464	1.34	171	50[1] ($at4$)	Yes

[1]Test time terminated by arrival of driver gas interface (calculated using L1d).
[2]Test time terminated by pressure drop due to arrival of $u + a$ wave.

Figure 8 shows experimental results for Shot ID #5 (refer Table 1), which was without an orifice plate, superimposed on a corresponding one dimensional CFD prediction using the code L1d (Jacobs, 1998). It is seen that the CFD agrees well with the measurements, that the maximum steady test time is about 40 ms, and occurs near the location of pressure transducer $at3$. The test time at $at4$ is seen to be vanishingly short, as the $u - a$ wave cancels the pressure rise about 10 ms after the incident shock.

Figure 9 shows experimental results for Shot ID #7, *with* an orifice plate. The maximum test time is seen to last for about 50 ms, and occurs near the location of $at4$. Transducer $at4$ is approximately where the observation station would be positioned if using this configuration. Again, good agreement with CFD is observed, adding confidence that flow processes are understood, and that accurate flow properties can be calculated.

For the Shot #7 configuration, the test time is terminated by the arrival of the driver gas/test gas interface, which in Figure 9 has been computed from the CFD. Pressure and velocity are constant across this interface, which is why the static pressure level is observed to remain approximately constant for another 20 ms after the interface arrival. What changes across the interface is the temperature; the test gas has been shock processed and has therefore been compressively heated; the driver gas, initially at higher pressure, has been processed by an unsteady expansion, and has thus cooled. So the driver gas is denser than the test gas, it's properties are different to those of the

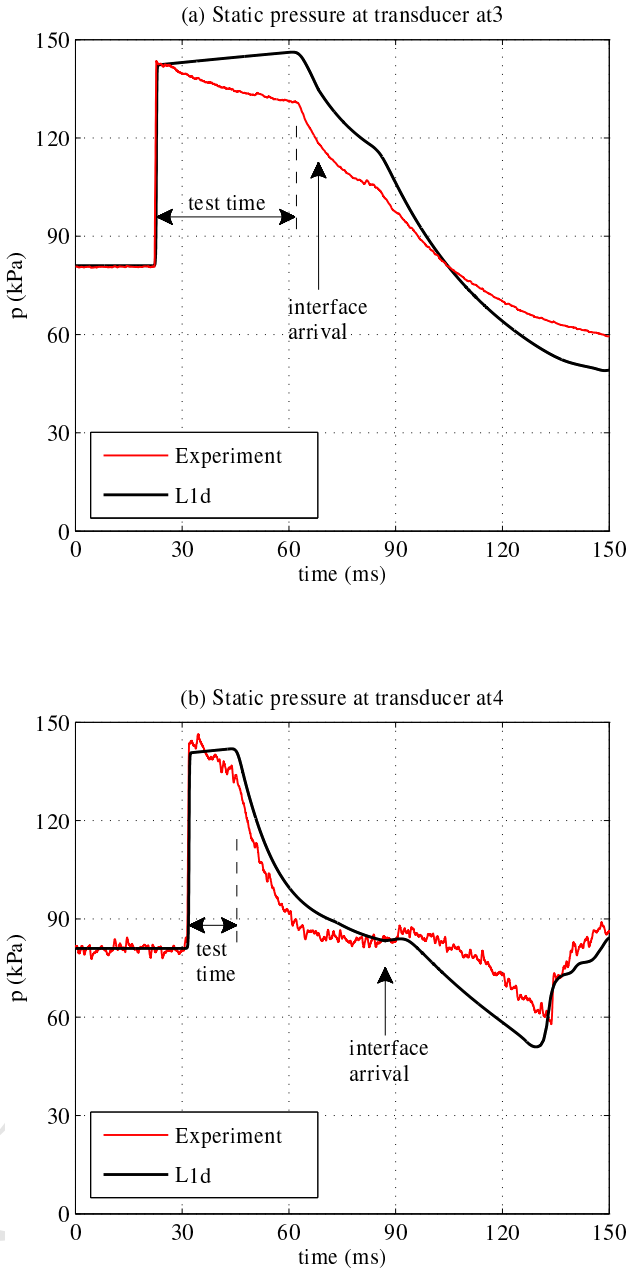

Figure 8: Results for Shot #5 (*without* orifice plate), showing experimental (red) and CFD (black) results. Maximum test time occurs close to *at*3, and terminates when the static pressure drops due to arrival of the *u*-*a* wave; the L1d computed interface arrival time is also shown. Experimental traces are time-referenced to L1d traces.

target flow condition, therefore it is not included in the test time calculation.

A disturbance is seen in the Figure 9 pressure trace about 12 ms after the arrival of the incident shock, which is due to the starting process of the orifice plate. The computed disturbance is more diffuse than the experiment; this is attributed to the 1D Lagrangian CFD model, which must model the orifice as a ramped area change over a finite length, as opposed to a discrete change in the actual facility (refer Figure 10).

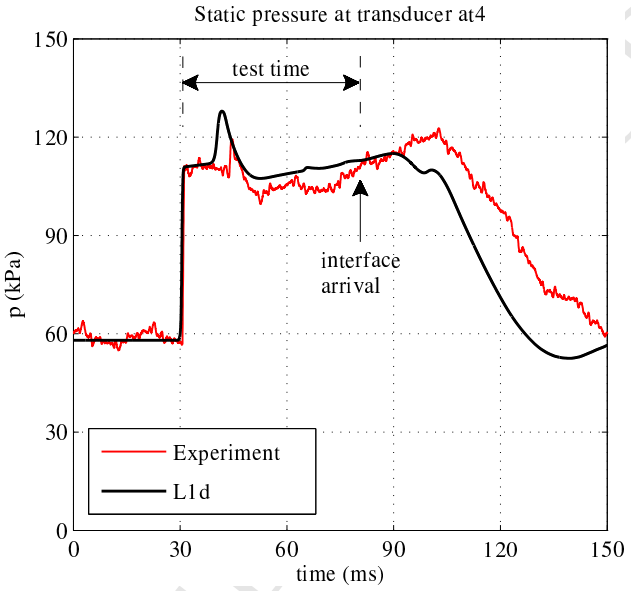

Figure 9: Results for Shot #7 (without orifice plate), showing experimental (red) and CFD (black) results. Maximum test time occurs close to *at*4, and terminates with arrival of the driver gas interface (computed using L1d). Experimental trace is time-referenced to L1d trace.

Figure 11 is an x-t diagram showing the progress of the shock along the tube, in terms of the arrival time of the shock at each respective pressure transducer. Results are time-referenced to the beginning of the L1d CFD simulation. Figure 12 shows the average shock speed along the tube, calculated based on the time of flight between transducer pairs. Observing both plots, it is noted that the shock attenuation is low, and that CFD agrees well with the measurements.

Error bars are shown for the experimental shock speed calculations in Figure 12; uncertainty is $\pm 1\%$ at each location except between transducers

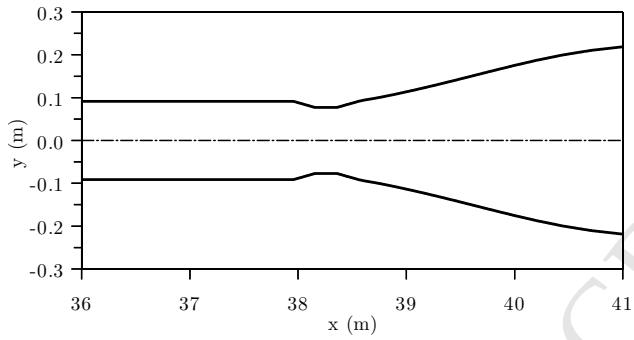

Figure 10: Orifice geometric representation in L1d CFD model.

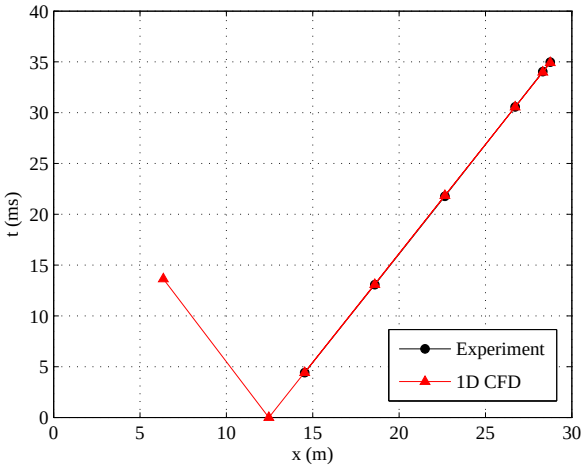

Figure 11: Progress of shock wave and unsteady expansion along tube for Shot #7 (shock arrival time versus axial distance), showing experimental (red) and CFD (black) results.

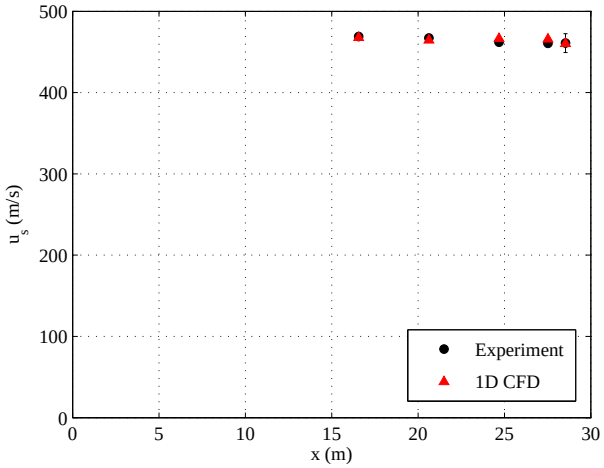

Figure 12: Development of shock speed along tube for Shot #7, showing experimental (red) and CFD (black) results.

$at6$ and $at7$, where it rises to $\pm 2.5\%$ due to the close proximity of these transducers. In Figure 12 it is further noted that the speed of the unsteady expansion propagating back into the driver tube after rupture is not calculated for the experiment. This is because the unsteady expansion arrives as a diffuse wave, not as a shock discontinuity, and its exact onset is difficult to identify from the experimental traces. In addition, the instrumentation used in that section was installed for hypervelocity measurements at much higher pressures, and are not ideal for the study of low pressure expansion waves. Quantification of wave speed in the driver does not affect the accuracy of measurements made in the test section, so optimised instrumentation was not installed, but could be if required for future test campaigns.

Figure 13 and Figure 14 show L1d CFD x-t diagrams for Shots #5 and #7 (respectively without and with an orifice plate). Contours of static pressure are mapped over the wave diagrams. The interface between the driver and test gases is the black line originating at $x = 12.8$ m. Referring to Figure 13, without an orifice plate the expansion from the dumptank is seen to accelerate the interface after $t = 65$ ms. Referring to Figure 14, when an orifice plate is used, the interface remains on a constant velocity trajectory. A small disturbance due to orifice plate flow start-up can be observed, characterised by a packet of waves travelling upstream from the orifice at $t = 30$ ms. These

waves are, however, weak and self-cancelling, as indicated by the minimal impact they have on the trajectory of the contact surface.

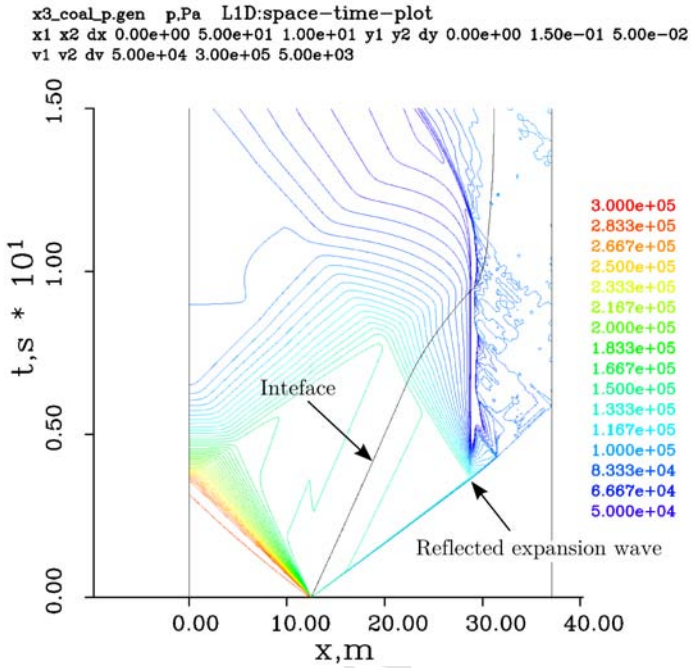

Figure 13: CFD x-t diagram and pressure contours for Shot #5 (*without* orifice; refer Table 1).

Figure 15 shows the computed static pressure for the Shot #7 initial fill conditions, for configurations *with* and *without* an orifice plate. In both cases, the static pressure is presented at the location of maximum test time for each configuration. Referring to Figure 14, these locations correspond to $x_1 = 22.7$ m for the case *without* an orifice plate, and $x_2 = 27.9$ m *with* an orifice plate. The black and red curves in Figure 15 show the respective static pressures at these two locations. The test times, which in both cases terminate with the arrival of the driver/test gas interface, are shown for both cases. It can be seen that the use of an orifice plate can extend the maximum available test time by 60%. Once again there is a disturbance observed with the orifice plate configuration (the red curve); in this fully optimised configuration, the disturbance arrives almost immediately after the test begins, which reflects the fact that the test section would be physically

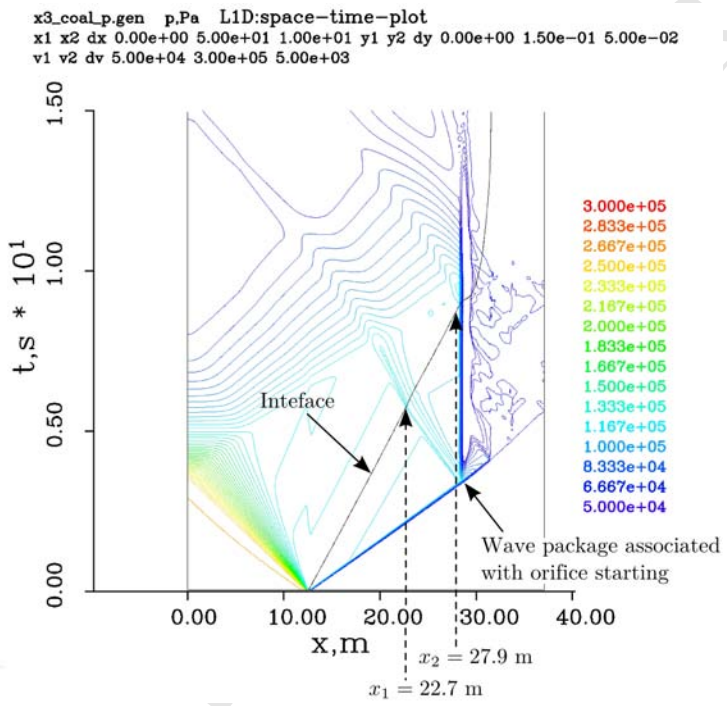

Figure 14: CFD x-t diagram and pressure contours for Shot #7 (*with* orifice; refer Table 1).

located immediately adjacent to the orifice plate.

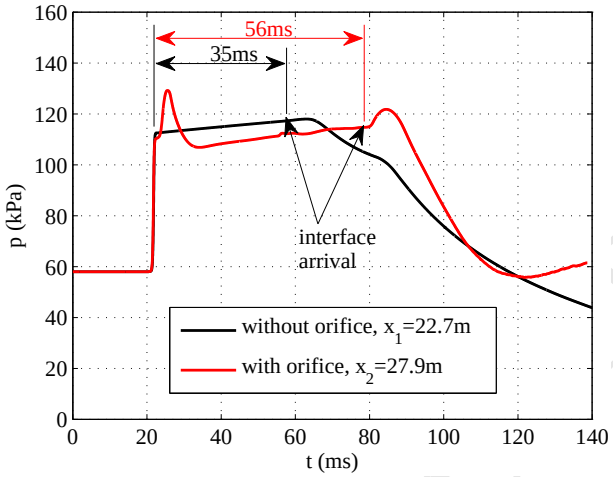

Figure 15: Computed static pressure at location of maximum test time, for shot Shot #7 initial fill conditions (refer Table 1), *with* and *without* an orifice plate. The black trace is for Shot #7 *without* an orifice plate, and shows the static pressure at $x_1 = 22.7$ in Figure 14, which is the location of maximum test time for this configuration; the red curve shows the static pressure for Shot #7 *with* an orifice plate, and shows the static pressure at $x_2 = 27.9$, which is the location of maximum test time for the case *with* an orifice plate. Note: the red curve has been time referenced to the black curve. The orifice plate is predicted to provide 21 ms (60%) additional test time, which in both cases terminates with arrival of the driver/driven gas interface.

8. Advantages of Using the Orifice Plate

The primary purpose of the orifice plate is to form a sonic throat at the exit of the tube. This prevents reflection of an unsteady expansion wave upstream, and would thus allow a test section to be located at the end of the tube, where test time is a maximum. If this configuration is adopted, the test section should therefore be located just upstream of the orifice plate.

This arrangement is convenient because it establishes a fixed location for the test section, which will not vary across the range of conditions of interest in this type of study. The end of a tube is also a convenient location to locate and service a test section.

Another advantage of the orifice plate arises from its decoupling of flow processes further downstream. If a minimally thin diaphragm were used to

seal the orifice exit, it would no longer be necessary to exhaust the shock tube into a dump tank at the same initial pressure as the shock tube. Instead, the tube could, for example, exhaust into atmospheric pressure. In this scenario, the diaphragm could have very light construction since it has a relatively small cross-sectional area, and for these types of conditions, only needs to support a fraction of an atmosphere pressure differential. Noting that stone dust is a messy medium to subject to explosive flow processes in the laboratory, larger scale dust lifting experiments in an outside facility could be exhausted into the open, or into a collection device for later analysis or disposal.

9. Conclusions

The first aim of this study was to propose a set of test requirements for certification of alternative stone dust products, such as slurry or foaming stone dust. It was concluded that such tests should involve the study of the dust lifting process which occurs behind shock waves of M =1.05–1.4, for respective test times of between 30 and 340 ms, and that the shock tube is a suitable facility for accurately reproducing these conditions. The two key characteristics of these proposed test flows are that they are associated with weak explosion scenarios, and they have longer test times than previous shock tube studies.

The efficacy of new products should be established by comparison to an equivalent dry stone dust application subject to the same tests. Such testing would only examine the dust lifting process which occurs between the passing of the shock and the arrival of the flame. Assuming that the dry stone dust application has already been approved for use, then it is argued that the explosibility does not need to be re-established for the alternative product. However, it may nevertheless be desirable to perform an independent validation of the new stone dust product using a detonation tube, to verify that the product can suppress the standard propagating explosion tests which these facilities produce.

The second aim of this study was to establish an optimised shock tube configuration to conduct the new tests. Preliminary experiments have confirmed that the X3 impulse facility can operate satisfactorily as a non-reflected shock tube to give good quality, long duration flows at low Mach numbers. The development of a new orifice plate concept enables full use of the shock tube length to be utilised, and test flows up to 60 ms have been

obtained (the actual test time will depend on shock Mach number selected). The starting process of the orifice plate causes a minor disturbance to propagate back through the subsonic shock-heated gas, which can be seen as noise in the test station.

The tunnel can be configured to produce any Mach number and ambient pressure level likely to be required for the study of explosions in mines. For each Mach number of interest, a different orifice plate has to be fabricated with throat area tuned for that condition. For the observation of post-shock phenomena, a window section must be installed in the shock tube, at an axial station located for maximum steady test time duration. When an orifice plate is used, the test section would be located at the tube exit, just upstream of the orifice plate.

10. Acknowledgements

The authors wish to thank: Mr F. De Beurs for technical support, and Applied Australia Pty Ltd for identifying the relevance of The University of Queensland's impulse facilities for studying the dust lifting process which occurs in coal dust explosions.

References

Abbasi, T., & Abbasi, S. (2007). Dust explosions - Cases, causes, consequences, and control. *Journal of Hazardous Materials*, *140(1–2)*, 8–40.

Anderson Jr., J. D. (1990). *Modern Compressible Flow with Historical Perspective*. (2nd ed.). McGraw-Hill Publishing Company, International Edition.

Cain, P. (2003). *The use of stone dust to control coal dust explosions: a review of international practice*. Rokdok, for The Stakeholders of the Federal Government / Industry Underground Coal Mines Safety Research Collaboration Administered by Natural Resources Canada, March.

Cashdollar, K. L., Sapko, M. J., Weiss, E. S., Harris, M. L., Man, C. K., Harteis, S. P., & Green, G. M. (2010). Recommendations for a new rock dusting standard to prevent coal dust explosions in intake airways. Report of Investigations 9679, in Department of Health and Human Services,

Centers for Disease Control and Prevention, National Institute for Occupational Safety and Health, Office of Mine Safety and Health Research, Pittsburgh, PA.

Cybulski, W. (1975). *Coal dust explosions and their suppression*. Warsaw, Poland: Foreign Scientific Publications Department of the National Center for Scientific, Technical, and Economic Information (translated from Polish).

Dastidar, A. G., Amyotte, P. R., & Pegg, M. J. (1997). Factors influencing the suppression of coal dust explosions. *Fuel*, *76(7)*, 663–670.

Gerard, J. H. (1963). An experimental investigation of the initial stages of the dispersion of dust by shock waves. *Brit. J. Appl. Phys.*, *14*, 186–192.

Harris, M. L., Weiss, E. S., Man, C. K., Harteis, S. P., Goodman, G. V., & Sapko, M. J. (2010). Rock dusting considerations in underground coal mines. In *Proceedings of the 13th U.S./North American Mine Ventilation Symposium, Sudbury, Ontario, Canada, June 13–16*.

Humphreys, D., Collecutt, G., & Proud, D. (2010). CFD simulation of underground coal dust explosions and active explosion barriers. In *Proceedings of the 10th Underground Coal Operators' Conference, University of Wollongong & the Australasian Institute of Mining and Metallurgy, pp. 330–338*.

Humphreys, D., & OBeirne, T. (2000). Risk assessment based stone dusting and explosion barrier requirements. In *Proceedings of the Queensland Mining Industry Health and Safety Conference, Townsville, Queensland, Australia, August 27–30*.

Jacobs, P. A. (1998). *Shock Tube Modelling with L1d*. Research Report 13/98, Department of Mechanical Engineering, The University of Queensland, November.

Klemens, R., Zydak, P., Kaluzny, M., Litwin, D., & Wolanski, P. (2006). Dynamics of dust dispersion from the layer behind the propagating shock wave. *Journal of Loss Prevention in the Process Industries*, *19*, 200–209.

Liebman, I., Duda, F., & Conti, R. (1979). Sensortrigger device for explosion barrier. *Rev. Sci. Instrum.*, *50(11)*, 1441–1444.

Man, C. K., & Teacoach, K. A. (2009). How does limestone rock dust prevent coal dust explosions in coal mines? *Mining Engineering*, *61(9)*, 69–73.

Marks, B., Chowdhury, A., Petersen, E., & Mannan, M. (2013). A new facility for studying shock-wave passage over dust layers. In *Proceedings of the 29th International Symposium on Shock Waves, Madison, Wisconsin, USA, 14–19 July*.

Mining Mirror (2013). Research facilitating foaming. *Mining Mirror, May*, (pp. 26–31).

NIOSH (2006). *Float Coal Dust Explosion Hazards*. Milestones in Mining Safety and Health Technology, No. 515, April. U.S. Department of Health and Human Services, Centers for Disease Control and Prevention, National Institute for Occupational Safety and Health, DHHS (NIOSH), Publication No. 2006-125, *http://www.cdc.gov/niosh/mining/UserFiles/works/pdfs/2006-125.pdf*.

NSW DPI (2001). *Guideline for coal dust explosion prevention and suppression, MDG-3006-MRT5*. New South Wales Department of Primary Industries (NSW DPI), Mine Safety Operations Division, December.

Oberholzer, J. W. (1997). *Assessment of Refuge Bay Designs in Colleries*. Safety in Mines Research Advisory Committee SIMRAC Final Project Report COL 115.

Oberholzer, J. W., Bennett, A. T., & Davis, R. L. (2005). *Effectiveness of Slurry Stone Dusting in Preventing the Progression of Underground Explosions*. Australian Coal Association Research Program (ACARP), ACARP Project Number No C13023, October.

OMSHR (2014). *Mining Topic: Rock Dusting*. Office of Mine Safety and Health Research (OMSHR), `http://www.cdc.gov/niosh/mining/topics/RockDusting.html`, accessed 24 Jan 2014.

Sapko, M. J., Weiss, E. S., Cashdollar, K. L., & Zlochower, I. A. (2000). Experimental mine and laboratory dust explosion research at NIOSH. *Journal of Loss Prevention in the Process Industries*, *13(3)*, 229–242.

Sichel, M., Kauffman, C. W., & Li, Y. C. (1995). Transition from deflagration to detonation in layered dust explosions. *Process Safety Progress*, *14(4)*, 257–265.

Singer, J. M., Harris, M. E., & Grumer, J. (1976). *Dust Dispersal by Explosion-Induced Airflow: Entrainment by Airblast*. Pittsburgh Mining and Safety Research Center, Pittsburgh, Pa., Report of Investigations 8130, United States Department of Interior / Bureau of Mines.

Stephan, C. (1998). *Coal Dust Explosion Hazards*. Mine Safety and Health Administration. Washington, D.C., *www.msha.gov/s&hinfo/techrpt/p&t/coaldust.pdf*.

Suzuki, T., Sakamura, Y., Igra, O., Adachi, T., Kobayashi, S., Kotani, A., & Funawatashi, Y. (2005). Shock tube study of particles' motion behind a planar shock wave. *Meas. Sci. Technol.*, *16*, 2431–2436.

Woskoboenko, F. (1988). Explosibility of victorian brown coal dust. *Fuel*, *67(8)*, 1062–1068.

Wu, H. W., Gillies, A. D. S., Oberholzer, J. W., & Davis, R. (2009). Australian Sealing Practice and use of Risk Assessment Criteria - ACARP Project C17015. In *Proceedings of the Queensland Mining Industry Health and Safety Conference, Townsville, Queensland, Australia, August 23–26*.